



AENSI Journals

Australian Journal of Basic and Applied Sciences

ISSN:1991-8178

Journal home page: www.ajbasweb.com



## Comparative Studies of Heat and Mass Transfer by Convective and Microwave-Convective Drying for Nonhygroscopic Ceramic

<sup>1</sup>Zawati Harun and <sup>2</sup>Tze Ching Ong

<sup>1</sup>Associate Professor, University Tun Hussien Onn, Advanced Manufacturing and Materials Center (AMMC), Faculty of Mechanical and Manufacturing Engineering, Parit Raja, 86400, Batu Pahat, Johor, Malaysia

<sup>2</sup>PhD candidate, University Tun Hussien Onn, Advanced Manufacturing and Materials Center (AMMC), Faculty of Mechanical and Manufacturing Engineering, Parit Raja, 86400, Batu Pahat, Johor, Malaysia

### ARTICLE INFO

#### Article history:

Received 15 September 2014

Accepted 5 October 2014

Available online 25 October 2014

#### Keywords:

Nonhygroscopic, ceramic, convective, microwave, drying, mathematical model,

### ABSTRACT

Drying is a complex process as it involves a lot of mechanism and material process particular heat and mass transfer that evolves concurrently during the process. In a simple word drying can be defined as removal of water or moisture from any porous substances. Drying may be accomplished by convective heat transfer, conduction from heated surfaces, by radiation or by dielectric heating. Different drying technique also will result in the different structure and properties of the dried or sinter body since moisture removal has strong correlation with shrinkage, packing porous structure as well as pore formation. Thus, understanding drying mechanisms under different drying techniques can help to control failure of the dried product. This aim of this paper is to propose a mathematical model and compare the drying mechanism for both convective and microwave-convective drying for nonhygroscopic ceramic materials. This current work used a coupled mathematical model of mass, heat and gas transfer that embedded with finite element method in two-dimensional domain and numerically computed using Skyline solver to capture highly nonlinear transient process. The model variables which provide analysis of time evolution of saturation, temperature and gas pressure are used to obtain better understanding of the mechanism that occur during the process of drying at fundamental level. Validation of the proposed model shows good agreement with the experimental data and other model results gained elsewhere. The computed results showed effectiveness of the drying process improves drastically in convective-microwave drying when compared to convective drying corresponding to mass and heat fluxes coincide in same direction, where from internal of matrix to the surface material. Thus easier removal of moisture is noted with higher temperature, moisture saturation and gas pressure accumulated at the bottom center of the material. However, the combination of those gradients may also lead to increment in potential internal defects on the dried material. Nevertheless, the increase understanding in fundamental mechanism that occurs during both drying modes is acknowledged resulted from the proposed model.

© 2014 AENSI Publisher All rights reserved.

**Cite This Article:** Zawati Harun and Tze Ching Ong., Comparative Studies of Heat and Mass Transfer by Convective and Microwave-Convective Drying for Nonhygroscopic Ceramic. *Aust. J. Basic & Appl. Sci.*, 8(15): 218-225, 2014

## INTRODUCTION

Various materials undergo drying process in the industries. Drying process involves moisture migration from the internal of the porous matrix to the external surrounding environment which occurs through one or more mechanism (Haghi, 2006; Harun and Gethin, 2008; Perré, P, *et al.*, 2007). This process is further complex via sophisticated as it is highly influences by the material properties and characteristic of the dried material. Thus, drying rates are unique between each configurations of drying process in regards to the drying methods and dried materials itself. Production efficiency which associate with time, cost, energy consume and quality of final product are closely interrelated with the drying rate of the selective drying method (Mujumdar, 2006). Hence, in order to optimize all those aforementioned parameter, the combination of drying methods with different sources of energy supply are more preferable when compared to traditional convective method.

The main aim of this paper is to present a proposed mathematical model of heat and mass transfer for both convective and convective-microwave drying and its validation with experimental data and other model results gained elsewhere. The proposed heat and mass transfer in this model may show combination of the different

**Corresponding Author:** Tze Ching Ong, PhD candidate, University Tun Hussien Onn, Advanced Manufacturing and Materials Center (AMMC), Faculty of Mechanical and Manufacturing Engineering, Parit Raja, 86400, Batu Pahat, Johor, Malaysia.  
Tel: 60198873615; E-mail: alex\_ongtc@yahoo.com

methods of drying which expect to bring positive output in shortening the drying duration and better quality of the dried products. Convective drying is often use in many material industries such as wood (Perré and Turner, 1999), fruit (Wang & Chen, 1999), fabric (A K Haghi, 2003) and others. The commonly known advantage of the convective drying when compared with others methods is its relative low cost as often associated to ambient or natural drying condition. However, the significant drawbacks are longer drying duration and low quality of dried products. Thus, new drying methods which can offer better production time and quality are becoming a necessity in many related industry. Therefore, large efforts to tackle such problems associated with convective drying generate worldwide interest. Lately, studies that involve combination of the drying methods have gained increase attention due to many advantages.

Recently, the concept of microwave drying has been intensively used for drying a wide variety of materials and applications. Internal heating that offers by microwave drying results in lower consumption of energy, better structure of dried products of mechanical strength or biological value is seems to the answer of improving the efficiency of the convective drying (Turner *et al.*, 1998). Convective-microwave in ceramic drying process conducted by Kowalski *et al.*, 2010 has shown a rapid improvement in the effectiveness of the drying process via time and quality of the dried material. However also, experimental works conducted by Kowalski *et al.*, 2012 on microwave drying using varies microwave power shows material may suffer destruction and shrink effect caused by the induced stress works especially of high power configuration. This showed the microwave heating is intensively related to the microwave power supplied as the rapid heating cause sudden moisture gradient from internal towards the material surface and further towards surrounding. This phenomenal often causes internal destruction resulted from internal overpressure and this may cause various gradients effect from different evolve variables during the drying process (Kowalski *et al.*, 2012). Therefore, the fundamental analysis of heat and mass transfer phenomena involving the gradient that dominant during the different phase of the drying process is crucially needed in conducting studies of drying works.

Comprehensive modeling of convective-microwave drying has been thoroughly treated in the past (Ni *et al.*, 1999; Ratanadecho *et al.*, 2001; Sanga *et al.*, 2002). As noted in those works, a very complex heat and mass transfer process arises during the drying process due to the nature of the process and complicated structure of the porous material itself. These complications result a complex mathematical formulation to represent the details of the physical phenomena associated with the process. However, due to its advantages such as increase in drying rates and faster drying times that offered by the process has attract many detail investigation in improving and extending this drying technique especially when there is limited research in area of convective-microwave in ceramic membrane preparation.

In this present works, the former convective model presented by Z Harun and Gethin, 2008; Z Harun and Ong, 2014; Zawati Harun *et al.*, 2014 is modified and extended to suit with the proposed drying method. In this proposed model, the work from previous study will be revised to implement the coupled mass, heat and gas transfer in two-dimensional domain for nonhygroscopic porous materials using a more rigorous mathematically microwave heating model which is embodied after careful studied. The main moisture migration transport mechanism are due to liquid flow by capillary action, vapor by diffusion and gas by vapor diffusion and bulk air flow in convective-microwave drying phenomena were taken into consideration in this model. The next section of this paper will discussed in detail the development of the mathematical model. To instill the confidence in the proposed model, the computed results will be validated extensively with experimental data and others models gained elsewhere. (Turner *et al.*, 1998; Stanish *et al.*, 1986)

### Theoretical Formulation:

General mass and energy conservation law are used to define the mechanism of mass and heat transfers during the drying process in this model. The hydraulic transports of the drying are represents liquid by capillarity action, diffusion by vapor and air. The three measured system variables are water pressure  $P_l$ , temperature  $T$  and gas pressure  $P_g$ .

$$\frac{\partial(\phi_l S_l)}{\partial t} + \frac{\partial(\phi_v S_g)}{\partial t} = -\nabla \cdot (\rho_l V_l) - \nabla \cdot (\rho_v V_v) - \nabla \cdot (\rho_g V_g) \quad (1)$$

The water velocity,  $V_l$  and gas velocity,  $V_g$  can be easily derived from Darcy's law as (A. K. Haghi, 2006):

$$V_l = -K_l [\nabla(P_l + Z)] \quad (2)$$

$$V_g = -K_g [\nabla P_g] \quad (3)$$

where,  $K_l$  denotes the hydraulic conductivity of water,  $K_g$  is the hydraulic conductivity of gas and  $Z$  is the vertical elevation from a datum (positive upward). Also noted from eq. (3), effect of gravity is significant in liquid flow but not for gas flow. Meanwhile vapor velocity by diffusion is defined as (Kanno *et al.*, 1996);

$$V_v = \frac{-D_{am} \nabla \theta_a}{\rho_v} \cdot \nabla \rho_v \quad (4)$$

where  $D_{am}$  denotes the molecular diffusivity of water vapour through dry air,  $\alpha$  is the tortuosity factor,  $\nu$  is a mass flow factor and  $\theta_a$  is the volumetric content of the air. In this work, the molecular diffusivity of water vapour through dry air is taken from the works of Stanish *et al.*, 1986 as:

$$D_{am} = 2.20 \cdot 10^{-5} \left( \frac{101325}{P_a + P_v} \right) \left( \frac{T}{273.15} \right)^{1.75} \quad (5)$$

The expression used in this study for the mass flow factor  $\nu$  was introduced by Philip and De Vries, 1957 and they suggested the use of an expression proposed as:

$$\nu = \frac{P_g}{P_g - P_v} \quad (6)$$

where  $P_v$  denotes the partial pressure of vapour and can be calculated from,

$$P_v = \rho_v R_v T \quad (7)$$

The tortuosity factor is set to a fix value of 0.5 for both horizontal and vertical axis in ceramic structure. Rearranging the above equation according to the measured variables gives;

$$V_v = \frac{-D_{am} \nu \alpha \theta_a}{\rho_v} \left\{ \rho_o \frac{\partial h}{\partial P_l} \nabla P_l + (\rho_o + h\beta) \frac{\partial h}{\partial T} \nabla T + \rho_o \frac{\partial h}{\partial P_g} \nabla P_g \right\} \quad (8)$$

By applying a mass balance to the flow of dry air within the pores of the material body dictates that the time derivative of the dry air content is equal to the spatial derivative of the dry air flux.

$$\frac{\partial(\phi \rho_a S_g)}{\partial t} = -\nabla(\rho_a V_g - \rho_v V_v) \quad (9)$$

The only effect of microwave towards the material is that they generate heat inside the material. Thus, the conduction, latent heat, convection and volumetric heat supply are considered in the energy equation as given as below;

$$\frac{\partial((1-\phi)c_p \rho_s + \sum_{i=a,l,v} \phi s_i \rho_i c_i)}{\partial t} = \nabla(\lambda \nabla T) - \nabla(\rho_v V_v + \rho_v V_g) L - \nabla(\sum_{i=a,l,v} (T-T_r) \rho_i c_{pi} V_i) + \mathfrak{R} \quad (10)$$

where  $\mathfrak{R}$  denotes the volumetric heat supply due to absorption of microwave energy depends on water volumetric thermal conductivity and is expressed using a linear dependency of the absorbed microwave energy on moisture content by the following Kowalski *et al.*, 2010:

$$\mathfrak{R} = \rho_s (A + B X_l) \quad (11)$$

where  $A$  and  $B$  express the amount of microwave energy absorbed by the porous matrix and moisture respectively. For convective drying, we use similar equations as microwave-convective drying with the difference that this time,  $\mathfrak{R} = 0$ .

Furthermore, in order to get the set of equations for the drying model, a list of assumptions and restrictions is necessary. The following list is the assumptions and restrictions that are implemented to the current proposed model:

- i. The three phases, solid, liquid and gas phases within the porous structure are always exist in local thermodynamic equilibrium.
- ii. The fluid is consists of liquid and vapour phases.
- iii. The temperatures of the liquid and vapour phases in the body are equal at coincident arbitrary points due to movement of moisture in the porous skeleton is slow.
- iv. Ideal gas law applied to the gas phase that filled the pores and is a binary mixture of air and vapour.
- v. All dimensional changes that induced during drying are small and negligible. Hence, matrix is non-deformable.
- vi. Liquid is treated as non-bound water that is held nonhygroscopically within the solid phase.
- vii. The only effect of microwave is they generate volumetric heat source inside the material to be dried.
- viii. The matrix is rigid, homogenous and isotropic.
- ix. Porosity of matrix is uniform.
- x. Darcy's law applies to gas and liquid phases.
- xi. Stresses induced also insignificant and negligible.
- xii. Finally, hysteresis phenomena are ignored.

#### Thermodynamic Relationship:

The existence of a local equilibrium at any point within the porous is assumed. Kelvin's law is applied to the equation below.

$$h = \exp\left(\frac{P_w - P_g}{\rho_l R_v T}\right) \quad (12)$$

The vapour partial pressure can be defined as a function of local temperature and relative humidity where the saturation vapour pressure,  $\rho_o$  is estimated from Mayhew and Rogers, 1976 with saturated vapour density as a function of temperature as

$$\frac{1}{\rho_o} = 194.4 \exp\{-0.06374(T - 273) + 0.1634 * 10^{-3} (T - 273)^2\} \quad (13)$$

The degree of saturation,  $S$  is an experimentally determined function of capillary pressure and temperature.

$$S_l = S_l(p_c, T) \quad (14)$$

Saturation is expressed as combination of temperature effect [9] as in equation below.

$$S_l = \frac{\theta - \theta_r}{\theta_s - \theta_r} = \left(\frac{1}{1 + (\alpha \varphi(T))^n}\right)^m \quad (15)$$

where the parameters  $\alpha$ ,  $n$  and  $m$  are dependent of porous material properties and influence the shape of the water retention curve. The permeability of water and gas are based on Muelem's model (Baroghel-Bouny *et al.*, 1999) as

$$k_l(S_l) = \begin{cases} \sqrt{S_l(1 - (1 - S_l^{\frac{1}{m}})^m)^2} & S_l > S_{irr} \\ 0 & S_l < S_{irr} \end{cases} \quad (16a)$$

$$k_g(S_l) = \begin{cases} \sqrt{1 - S_l(1 - S_l^{\frac{1}{m}})^m} & S_l < S_{crit(g)} \\ 0 & S_l > S_{crit(g)} \end{cases} \quad (16b)$$

### Material Data:

Figure 1 shows the meshing of the sample in two-dimensional domain using eight-nodes quadratic quadrilateral element.

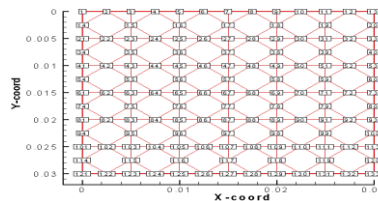


**Fig. 1:** Meshing of the rectangular sample.

The sample used is referred as a very thin rectangular slab of length  $L = 3\text{cm}$  and height  $H = 3\text{cm}$ . The slab was meshed with 36 elements and 133 nodes and is assumed to be a porous medium that is homogeneous, isotropic and composed of solid phase, water and vapor phase, gas phase and dry air phase. The initial saturation was set to be  $S_0 = 0.7$  and the initial temperature  $T_0 = 30^\circ\text{C}$ . The material properties and transport parameter used as data for simulation are listed in Table 1.

**Table 1:** Physical properties of ceramic body and transport parameter.

Density of porous matrix	$\rho_s$	$\text{kg/m}^3$	2000
Porosity	$\phi$	1	0.3
Intrinsic permeability	$K$	$\text{m}^2$	$10^{-16}$
Thermal conductivity of the porous matrix	$\lambda$	$\text{W/m K}$	1.8
Specific heat capacity of porous matrix	$C_p$	$\text{J/kg K}$	920
Critical saturation	$S_{cri}$	1	0.3
Irreducible saturation	$S_{irr}$	1	0.09
Constant denotes the absorption of microwave energy by skeleton (Eq. 11)	$A$	$\text{J/m}^3\text{s}$	126
Constant denotes the absorption of microwave energy by moisture (Eq. 11)	$B$	$\text{J/m}^3\text{s}$	20

### Boundary Condition:

To reflect the drying condition in convective-microwave drying chamber, the boundary conditions for mass and heat transfer were chosen as follows:

$$J_m = h_m (P_\infty^v - P_s^v) \quad (17)$$

$$J_T = h_c (T_\infty - T_f) \quad (18)$$

The boundary conditions of both drying modes are applied to the top and side surfaces of the sample while the lower bottom surface is impermeable and insulated for heat and moisture flow. Also top and side surfaces are assumed to remain under atmospheric condition. The ambient temperature is set at 30 °C with heat and mass coefficient of 20 W/m<sup>2</sup>K and 0.00164 ms<sup>-1</sup>. The maximum temperature in whole volume of the slab is set equal to the boiling water temperature corresponding to water as the main absorption medium of microwave energy in microwave-convective drying. Similar configuration is used for convective drying with the difference that the heat flux is pointed from outside to inside. The change of heat flux direction is implemented by multiplying both side of Eq. 18 by minus 1.

#### Solution Of Governing Equations And Numerical Method:

The two dimensional transient nonlinear coupled heat and mass transfer equations described above are written in the form of a matrix as follows;

$$[C(\Phi)] \frac{\partial}{\partial t} \{\Phi\} = \nabla([K_{cx}(\nabla\Phi)]i_x + [K_{cy}(\nabla\Phi)]i_y) \{\Phi\} + R(\nabla Z) \quad (19)$$

where  $\{\Phi\} = \{P_w, T, P_g\}$  is the column of unknowns;  $[C]$ ,  $[K_{cx}]$  and  $[K_{cy}]$  are 3x3 matrices. Each element of the matrix is a coefficient for the unknown  $\{\Phi\}$ ;  $i_x$  and  $i_y$  are the unit direction vectors. In order to discretize this simplified second order non-linear coupled partial differential equation, finite element method is used. Afterwards, Galerkin method is used to minimize the residual error before the application of Greens theorem, to the dispersive term involving second order derivatives; this simplified combined equation set can be expressed in the following form.

$$\underline{K}(\Phi)\Phi + \underline{C}(\Phi)\dot{\Phi} + \underline{J}(\Phi) = \{0\} \quad (20)$$

The transient matrix and nonlinear second order differential equations above are then solved by using a fully implicit backward time stepping scheme along with a Picard iterative method which is taken into account for non-linearity.

## RESULTS AND DISCUSSION

The first aim of this section is to compare the drying results computed by the proposed model with the experimental data and other models results. The validation of current model with the previous experimental data and computed results by Turner *et al.*, 1998 for microwave-convective drying and Stanish *et al.*, 1986 for convective drying are present in Figure 2.

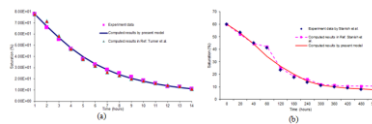


**Fig. 2:** Comparison of drying curve: (a) microwave-convective; (b) convective.

Figure 2 shows a comparison results between the predicted proposed model, other's model and experimental data. As demonstrated in this figure that all the drying period are present for all times for both drying techniques respectively. The good adherence of results generated by the proposed model with experimental data and other model results simulates that the computed results presented in this paper are the proper ones.

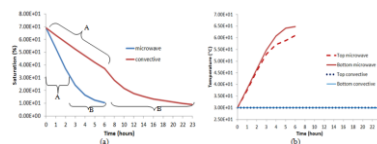


**Fig. 3:** Saturation (a) and temperature (b) curve with time for both drying modes.

Figure 3 depicts the temperature distribution and saturation evolution with time for both drying modes. The drying saturation curve is characterized with the straight segments in the constant drying rate periods (denotes by A in Figure 3(a)) and nonlinear curve in the falling rate period (denotes by B in Figure 3(a)). For microwave-convective drying, temperature arises abruptly due to the heat generation from the microwave energy directly heated the internal moisture volumetric across the bodies. Then sample temperature begin to rise drastically at constant rate period corresponding to volumetric heat as energy is transferred directly to the whole volumetric

liquid with homogenous distributed throughout the wet material. This mechanism also very profitable to moisture transport as depicted in Figure 3 also saturation decreasing rate is constant. This is mainly generated by the interior heat fluxes provide higher fluxes of liquid to surface from the interior of the material. Subsequently, when saturation level reaches the critical water content which is 0.3 for ceramic materials, the water rapidly changes into vapour phase. Consequences from declining saturation level, the temperature rising profile also decrease which water is the main absorption of the heat energy by microwave when reaches the falling rate period. Eventually, when saturation decrease gradually to the irreducible value where no water can be dried indicating the end of a drying condition. Temperature profiles also show no increment with decreasing of moisture content is decreasing as little heat energy is produced. Meanwhile during convective drying, saturation curve also illustrated all those aforementioned drying period but with significant slower rates due to colliding heat and mass transfer. Also noted, the surface material temperature for microwave-convective drying is less than the center of the material due to the volumetric heat generated is proportional with the moisture content and this phenomenal is conversed with the convective drying method where minimal temperature difference between surface and center of material is noticed. The contour evolution of convective-microwave drying on saturation and temperature distribution inside porous matrix will be further discussed and analyzed in detail when compare to the convective drying.

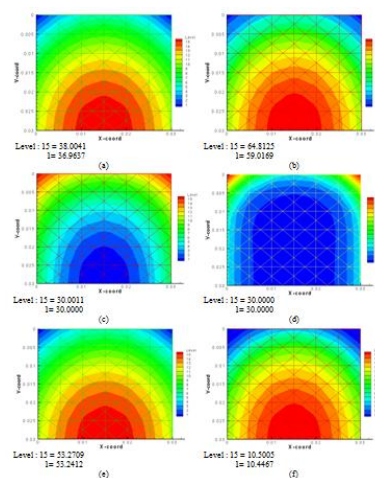


**Fig. 4:** Contour of saturation and temperature: (a) temperature at 1 hour for microwave-convective drying; (b) temperature at 6 hour for microwave-convective drying; (c) temperature at 1 hour for convective drying; (d) temperature at 23 hour for convective drying; (e) saturation at 1 hour for microwave-convective drying; (f) saturation at 6 hour for microwave-convective drying.

Heat supplied volumetrically leads to the different distribution of temperature obtained for convective-microwave drying as shown in Figure 4(a) and 4(b). This temperature distribution is accordance with experimental visualized distribution due to infrared camera measurement as presented in Kowalski *et al.*, 2012. This mechanism generated bulk heating phenomena inside the porous matrix. As can be noticed, the highest temperature is generated around the bottom center of the rectangular sample when microwave enter the rectangular sample through the lateral and upper surface. This corresponding to the accumulated moisture in the bottom center of the slab is due to the gravity effect. The distribution of temperature gained in convective-microwave drying is very profitable for moisture removal as the heat and mass fluxes coincide, which is contradict in convective drying where the fluxes moves in the opposite direction. This also eventually leads to easier moisture removal and is purely shown in the Figure 4(e) and (f) which illustrates the distribution of saturation content in the sample at early and end stage of drying. As it is visible in this figure, the highest saturation is also at the bottom center of the rectangular sample and the lowest one is in the top side corner. This indicates the most intensive part of the free mass transfer takes place at the top side corner of the rectangular sample. This is due to ability of water to absorb microwave energy provides an advantage compare convectional convective drying mode. Conversely to convectional convective drying mode where heat is transfer from the ambient to the surface material then to the interior of the material relies mainly on the conduction and convection propagation (refer Figure 4(c) and 4(d)), in microwave drying the heat is generated within the accumulated liquid inside interior of the material itself. Thus, this leads to more uniform moisture distribution, reducing drying time as drying rate increase abruptly from this mechanism. Nevertheless, saturation contours for convective drying are similar to microwave-convective drying, thus not is not presented in here.

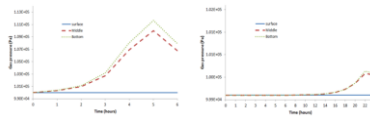


**Fig. 5:** Gas pressure evolution in time: (a) microwave-convective drying; (b) convective drying .

Figure 5(a) shows the gas pressure evolution in time at different positions inside the domain for convective-microwave and convective drying modes. As illustrated, the gas pressure slowly build up at the constant rate period of the drying process where moisture content is high inside pores at initial stage and capillary mechanism is the main supply of moisture from internal to surface material for evaporation to happen. When the drying stage reaches the falling rate period, pressure build up more drastically due to diffusion of vapour cause by phase transition change of water to vapor. Subsequently, gas pressure recede to atmosphere condition drop as drying is almost accomplished. As noted in figure 5, the surface of material remains constant at atmosphere pressure and higher internal pressure buildup within internal of the material. Figure 5 also demonstrated higher gas pressure occurs during microwave-convective drying when compared to convective drying. Subsequently the gas pressure gradient in the internal is high at the falling rate period which can cause internal damage in microwave-convective drying as proven in experiment by Kowalski *et al.*, 2012 that showed microwave tend to exhibit internal cracking compare to convective drying. Thus, controlling the drying rate for convective-microwave drying is vital to avoid failure in dried materials.

### Conclusion:

The results computed by the proposed model enable the investigation of fundamental mechanism for both convective-microwave and convective drying. It is noticed that the drying rates can increase drastically in convective-microwave drying compared to convective drying. To illustrate the above point, both heat and mass fluxes coincide in the same direction from internally to material surface as moisture removes continuously. Thus, both maximum temperature and saturation can be seen accumulated at the center bottom of the sample while top side surface exhibit lowest temperature and moisture content as the most profitable moisture extraction happen at this position. Also noted, the gas pressure is gathered at the same position and this could lead to overpressure internally. Lastly, this model is considered to be a useful tool for simulating the process of convective-microwave and convective drying process due to its reasonable accuracy at all times.

### Notations:

$T$  = Temperature, K

$P$  = pressure, Pa

$V$  = velocity,  $\text{ms}^{-1}$

$\rho$  = density,  $\text{kg/m}^3$

$S$  = saturation

$\emptyset$  = porosity

$C_p$  = specific heat capacity,  $\text{J}/(\text{mol K})$

$\theta$  = volumetric

$K$  = intrinsic permeability,  $\text{m}^2$

$k$  = relative permeability

$\lambda$  = thermal conductivity,  $\text{W/mK}$

$t$  = time, s

$R$  = gas constant,  $\text{J}/(\text{mol K})$

$\mu$  = viscosity,  $\text{N s m}^{-2}$

$h$  = relative humidity, %

$L$  = Latent heat of vaporization,  $\text{J kg}^{-1}$

$J_m$  = mass transfer flux

$J_T$  = heat transfer flux

$h_m$  = mass transfer coefficient

$h_T$  = heat transfer coefficient

$\Omega^e$  = element domain

$\underline{K}_{ij}$  = kinetic coefficients

$\underline{C}_{ij}$  = capacity coefficient

$N_r$  = Shape function of residual error

$N_s$  = Shape function of system variables

### Subscripts:

$a, c, v, g, l, b$  = air, capillary, vapour, gas, liquid, bound water

$s$  = saturated

$irr$  = irreducible

$cri$  = critical

$r$  = residual

$\infty$  = calculated

$f$  = final

### ACKNOWLEDGEMENTS

Authors thank to the financial support from University Tun Hussien Onn (UTHM) and KPTM.

## REFERENCES

- Baroghel-Bouny, V., M. Mainguy, T. Lassabatiere and O. Coussy, 1999. Characterization and identification of equilibrium and transfer moisture properties for ordinary and high-performance cementitious materials. *Cement and Concrete Research*, 29(8): 1225-1238.
- Haghi, A.K., 2003. Thermal Analysis of Drying Process: A theoretical approach. *Journal of Thermal Analysis and Calorimetry*, 74: 827-842.
- Haghi, A.K., 2006. Transport phenomena in porous media: A review. *Theoretical Foundations of Chemical Engineering*, 40(1): 14-26.
- Harun, Z. and D.T. Gethin, 2008. Drying Simulation of Ceramic Shell Build Up Process. 2008 Second Asia International Conference on Modelling Simulation AMS, 794-799.
- Harun, Z. and T.C. Ong, 2014. Material parameters sensitivity in modeling drying of porous materials. *Advanced Materials and Information Technology Processing*, 87: 91-98.
- Harun, Z., T.C. Ong, and R. Ahmad, 2014. Drying Comparison of Nonhygroscopic and Hygroscopic Materials. *Applied Mechanics and Materials*, 465: 637-641.
- Kanno, T., K. Kato and J. Yamagata, 1996. Moisture movement under a temperature gradient in highly compacted bentonite. *Engineering Geology*, 41(1-4): 287-300.
- Kowalski, S., J. Banaszak and A. Rybicki, 2012. Damage analysis of microwave dried materials. *AIChE Journal*, 58(7): 2097-2104.
- Kowalski, S., G. Musielak and J. Banaszak, 2010. Heat and mass transfer during microwave-convective drying. *AIChE Journal*, 56(1): 24-35.
- Mayhew, Y.R. and G.G.C. Rogers, 1976. *Thermodynamic and Transport Properties of Fluids*. Oxford: Blackwell.
- Mujumdar, A.S. (Ed.), 2006. *Handbook of Industrial Drying*. Boca Raton, USA: Taylor & Francis Group.
- Ni, H., A.K. Datta and K.E. Torrance, 1999. Moisture transport in intensive microwave heating of biomaterials: a multiphase porous media model. *International Journal of Heat and Mass Transfer*, 42: 1501-1512.
- Perré, P. and I. Turner, 1999. A 3-D version of TransPore: a comprehensive heat and mass transfer computational model for simulating the drying of porous media. *International Journal of Heat and Mass Transfer*, 42: 4501-4521.
- Perré, P., R. Remond, and I. Turner, 2007. Comprehensive drying models based on Volume Averaging: Background, Application and Perspective. In *Modern Drying Technology*, Eds., Tsotsas, E. and A.S. Mujumdar. Weinheim: Wiley VCH Verlag GmbH & Co. KGaA, pp: 1-12.
- Philip, J.R. and D.A. De Vries, 1957. Moisture movement in porous materials under temperature gradients. *Eos, Transactions American Geophysical Union*, 38: 222-232.
- Ratanadecho, P., K. Aoki and M. Akahori, 2001. A Numerical and Experimental Study of Microwave Drying Using a Rectangular Wave Guide. *Drying Technology*, 19(9): 2209-2234.
- Sanga, E.C.M., A.S. Mujumdar and G.S.V. Raghavan, 2002. Simulation of convection-microwave drying for a shrinking material. *Chemical Engineering and Processing: Process Intensification*, 41(6): 487-499.
- Stanish, M.A., G.S. Schajer and F. Kayihan, 1986. A mathematical model of drying for hygroscopic porous media. *AIChE Journal*, 32(8): 1301-1311.
- Turner, I., J. Puiggali and W. Jomaa, 1998. A numerical investigation of combined microwave and convective drying of a hygroscopic porous material: A study based on pine wood. *Chemical Engineering Research and Design*, 76(Part A): 193-209.
- Wang, Z.H. and G. Chen, 1999. Heat and mass transfer during low intensity convection drying. *Chemical Engineering Science*, 54(17): 3899-3908.